Supporting information for

Microbial colonization effects on drag in suspended sediment transport

Naiyu Zhang[1], Haochen Li[2], Fan Xu[1*], Charlie Thompson[3,4], Ian Townend[3], Qing He[1]

[1]State Key Laboratory of Estuarine and Coastal Research, East China Normal University, Shanghai, 200241, China

[2]Water Infrastructure Laboratory, Department of Civil and Environmental Engineering, University of Tennessee, Knoxville, TN 37996, USA

[3]School of Ocean and Earth Science, National Oceanography Centre, University of Southampton, Southampton, SO14 3ZH, UK

[4]Channel Coastal Observatory, National Oceanography Centre, Southampton, SO14 3ZH, UK

Corresponding author: Fan Xu (fxu@sklec.ecnu.edu.cn)

Introduction

This supporting information comprises:
Supplementary Text
Figs. S1 to S5
Table S1 to S2
References

Supplementary Text

Settling velocity experiments

Settling velocity experiments were conducted using a non-destructive video recording system (Laboratory Spectral Flocculation Characteristics instrument (LabSFLOC-2)) [1–3]. The LabSFLOC-2 system is a video recording system, that comprises a portable square Perspex settling column 350 mm in height, a digital camera to view the settling particles at the lower region of the column, a magnification lens, and a particle tracking and image processing system established upon the HR Wallingford Ltd DigiFloc software[4]. The LabSFLOC-2 system has been optimised for observing and tracking slow moving aggregates/particles, such as cohesive sediment flocs/oil-mineral aggregates, and was applied herein to measure the settling velocities of the slowly sinking clay and field muddy aggregates.

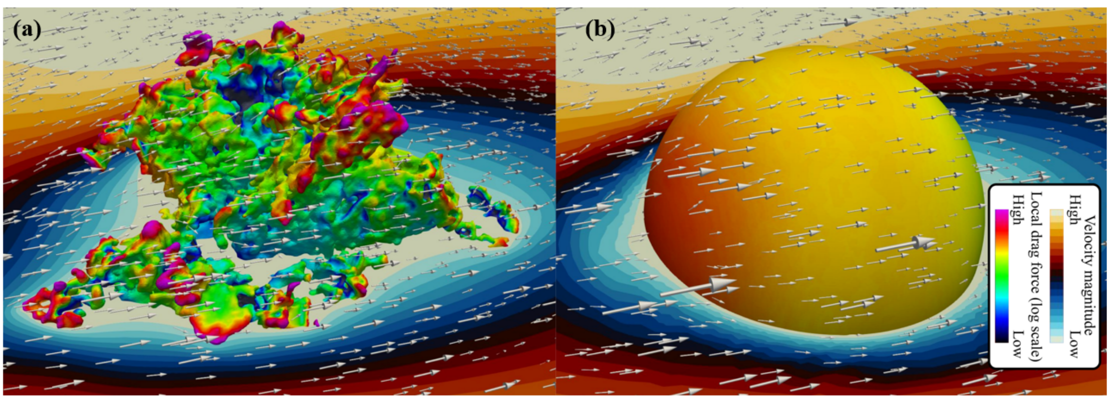

Figure S1.

CFD simulations of flow field around amorphous aggregates (a) and smooth spheres (b).

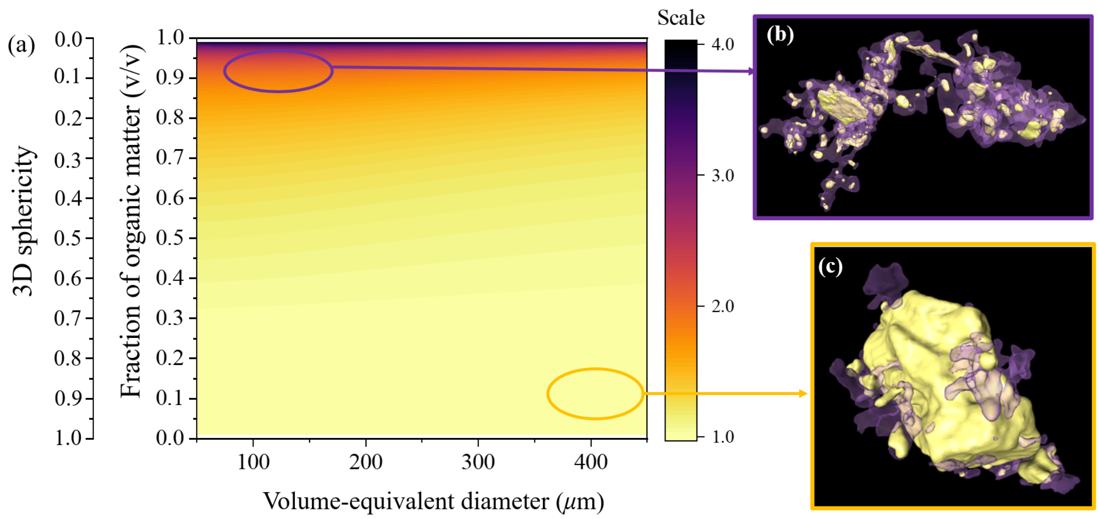

Figure S2.

Scale of settling velocity overestimates and its variance with the states of microbial colonization (a), with f_b increasing from 0 to 1 and 3D sphericity decreasing from 1 to 0. The settling velocity estimates were obtained by integrating our morphology-corrected drag law into settling velocity equation (). The dynamic interplay by size, density and aggregate morphology has different extents of positive and negative influences on settling for heavily and poorly-colonized aggregates, as conceptually illustrated in b and c, respectively.

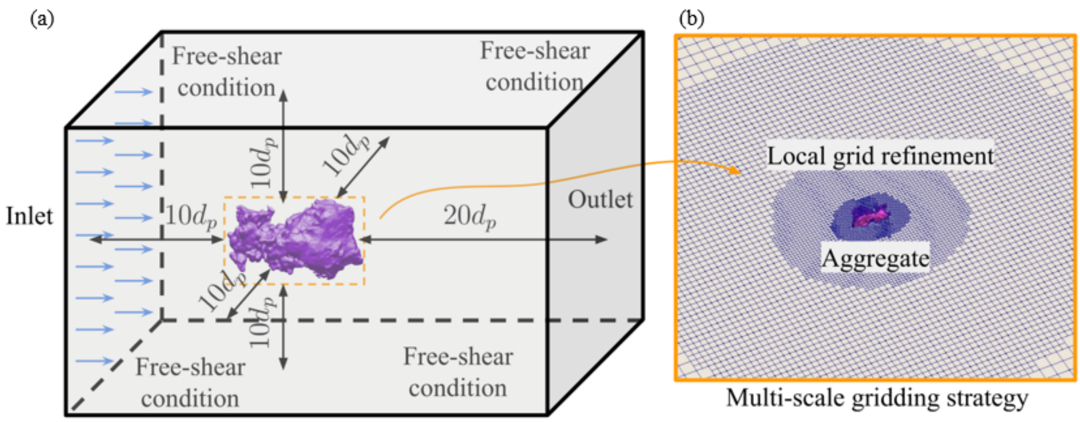

Figure S3.

CFD model configuration (a) and illustration of gridding strategy (b). *dp* is the aggregate diameter.

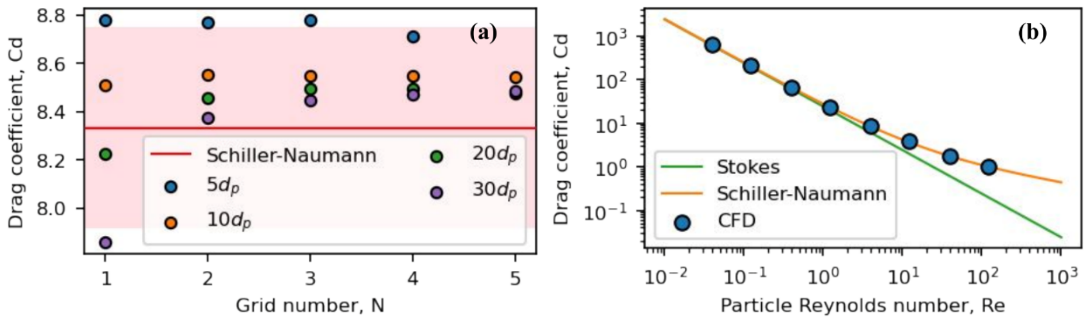

Figure S4.

Numerical convergence study with a sphere particle. (a) drag coefficient dependence on various grid configurations and mesh refinement; (b) comparison of CFD computed drag coefficient and Schiller-Naumann drag correlation.

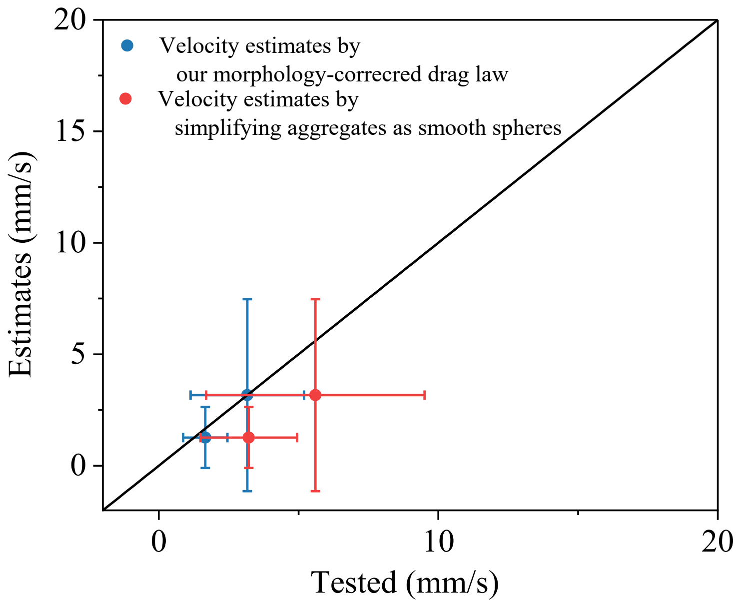

Figure S5.

Comparisons between the settling velocities estimated by our morphology-corrected drag law (blue dots) and that calculated by simplifying aggregates as smooth spheres (red dots) for clay aggregates created in laboratory and field muddy aggregates collected from the fluff layer on Hythe mudflat. These estimates (y axis) are plotted against experimental results (x axis).

Table S1

A summary of gross shape and normalized drag coefficient.

Corey Shape range	Parameter	N total	Mean	Standard deviation	Standard error of mean	Minimum	Median	Maximum
0.3-0.4	Corey shape factor	40	0.351	0.020	0.003	0.305	0.359	0.359
	Normalized drag coefficient	40	2.144	0.436	0.069	1.000	2.246	2.913
0.4-0.5	Corey shape factor	133	0.460	0.021	0.002	0.434	0.450	0.486
	Normalized drag coefficient	133	1.403	0.321	0.028	0.869	1.356	3.808
0.5-0.6	Corey shape factor	138	0.565	0.021	0.002	0.543	0.562	0.593
	Normalized drag coefficient	138	1.490	0.233	0.020	1.000	1.479	2.147
0.6-0.7	Corey shape factor	225	0.664	0.026	0.002	0.611	0.666	0.696
	Normalized drag coefficient	225	1.564	0.157	0.010	1.321	1.541	2.063
0.7-0.8	Corey shape factor	577	0.752	0.031	0.001	0.703	0.748	0.798
	Normalized drag coefficient	578	1.475	0.217	0.009	1.102	1.428	2.765
0.8-0.9	Corey shape factor	515	0.863	0.049	0.002	0.800	0.845	0.955
	Normalized drag coefficient	515	1.453	0.197	0.009	1.101	1.440	2.938

Table S2

A summary of 3D sphericity and normalized drag coefficient.

3D sphericity	Parameter	N total	Mean	Standard deviation	Standard error of mean	Minimum	Median	Maximum
0-0.1	3D sphericity	120	0.074	0.017	0.002	0.047	0.083	0.088
	Normalized drag coefficient	120	1.988	0.273	0.025	1.611	1.938	2.913
0.1-0.2	3D sphericity	714	0.163	0.026	0.001	0.118	0.169	0.198
	Normalized drag coefficient	714	1.547	0.209	0.008	1.007	1.538	3.808
0.2-0.3	3D sphericity	162	0.255	0.028	0.002	0.209	0.266	0.292
	Normalized drag coefficient	162	1.378	0.207	0.016	0.869	1.360	1.962
0.3-0.4	3D sphericity	338	0.360	0.026	0.001	0.314	0.358	0.396
	Normalized drag coefficient	338	1.425	0.123	0.007	1.219	1.416	1.781
0.4-0.5	3D sphericity	192	0.425	0.022	0.002	0.400	0.408	0.456
	Normalized drag coefficient	192	1.339	0.082	0.006	1.221	1.319	1.569
0.5-0.6	3D sphericity	102	0.533	0.015	0.001	0.516	0.530	0.554
	Normalized drag coefficient	102	1.216	0.067	0.007	1.109	1.212	1.365

References

1. Manning, A. J. LabSFLOC—a Laboratory System to Determine the Spectral Characteristics of Flocculating Cohesive Sediments. *In*: HR Wallingford Technical Report (HR Wallingford, 2006).
2. Manning, A. J., Friend, P. L., Prowse, N. & Amos, C. L. Estuarine mud flocculation properties determined using an annular mini-flume and the LabSFLOC system. Cont Shelf Res 27, 1080–1095 (2007).
3. Ye, L., Manning, A. J. & Hsu, T. J. Oil-mineral flocculation and settling velocity in saline water. Water Res 173, 115569 (2020).
4. Benson, T. & Manning, A. J. DigiFloc: The Development of Semi-Automatic Software to Determine the Size and Settling Velocity of Flocs. *In*: HR Wallingford Report (HR Wallingford, 2013).